World Academy of Science, Engineering and Technology
International Journal of Chemical and Molecular Engineering
Vol:12, No:10, 2018

Impact of Zn/Cr Ratio on ZnCrOx-SAPO-34 Bifunctional Catalyst for Direct Conversion of Syngas to Light Olefins

Yuxuan Huang, Weixin Qian, Hongfang Ma, Haitao Zhang, Weiyong Ying

***Abstract*—**Light olefins are important building blocks for chemical industry. Direct conversion of syngas to light olefins has been investigated for decades. Meanwhile, the limit for light olefins selectivity described by Anderson-Schulz-Flory (ASF) distribution model is still a great challenge to conventional Fischer-Tropsch synthesis. The emerging strategy called oxide-zeolite concept (OX-ZEO) is a promising way to get rid of this limit. $ZnCrO_x$ was prepared by co-precipitation method and $(NH_4)_2CO_3$ was used as precipitant. SAPO-34 was prepared by hydrothermal synthesis, and Tetraethylammonium hydroxide (TEAOH) was used as template, while silica sol, pseudo-boehmite, and phosphoric acid were Al, Si and P source, respectively. The bifunctional catalyst was prepared by mechanical mixing of $ZnCrO_x$ and SAPO-34. Catalytic reactions were carried out under $H_2/CO=2$, 380 ℃, 1 MPa and 6000 $mL \cdot g_{cat}^{-1} \cdot h^{-1}$ in a fixed-bed reactor with a quartz lining. Catalysts were characterized by XRD, N_2 adsorption-desorption, NH_3-TPD, H_2-TPR, and CO-TPD. The addition of Al as structure promoter enhances CO conversion and selectivity to light olefins. Zn/Cr ratio, which decides the active component content and chemisorption property of the catalyst, influences CO conversion and selectivity to light olefins at the same time. $C_{2-4}^{=}$ distribution of 86% among hydrocarbons at CO conversion of 14% was reached when Zn/Cr=1.5.

***Keywords*—**Light olefins, OX-ZEO, syngas, ZnCrOx.

I. Introduction

LIGHT olefins, consisting of ethylene, propylene, and butylene, are key chemicals. At present light olefins are mainly gained from naphtha cracking [1]. Syngas, a mixture of CO and H_2, is a vital platform for chemicals production via nonpetroleum route. Indirect conversion of syngas to light olefins has been industrialized, composing of methanol production and MTO (methanol-to-olefins) process. Meanwhile, Fischer-Tropsch (F-T) synthesis, which is the major path of syngas to light olefins, has been investigated for over 90 years [2]-[4]. However, the hydrocarbon distribution is still a challenge to its commercialization, as the ASF model shows that the carbon-based selectivity of light olefins is limited to less than 60%.

Recently, a strategy called OX-ZEO process was raised up with a high light olefins selectivity and little methane was formed [5]. According to the OX-ZEO process, CO and H_2 are activated over the partially reduced metal oxide, leading to the formation of CH_4 and intermediate. Subsequently, the intermediate participates the C-C coupling, which is controlled by zeolite pores with acidic sites. The nature of intermediate is still a matter of debate. Some authors pointed out that methanol or dimethyl ether is the intermediate [6], [7], which means the OX-ZEO process can be understood as the combination of methanol production and MTO process. Other authors proposed that ketene is the intermediate [5], [8].

Different oxides have been investigated, such as $ZnCrO_x$, $ZnO\text{-}ZrO_2$, $ZnGa_2O_4$, and MnO_x [5], [7], [9], [10]. $ZnCrO_x$ is used to produce light olefins and other organic products with different kinds of zeolite via OX-ZEO process, but the Zn/Cr ratio and its impact to catalytic performance has never been discussed [8], [11], [12]. Herein, we prepared $ZnCrO_x$ with different Zn/Cr ratio and investigated the impact of Zn/Cr ratio on the catalytic performance of bifunctional catalyst for direct conversion of syngas to light olefins. The addition of Al was also discussed.

II. Experimental Section

A. Catalyst Preparation

$ZnCrO_x$ oxide was prepared by coprecipitation method. Briefly, 22.31 g $Zn(NO_3)_2 \cdot 6H_2O$ and 20.01g $Cr(NO_3)_3 \cdot 9H_2O$ were dissolved in 125 mL deionized water and heated to 70 ℃. The solution was added to $(NH_4)_2CO_3$ solution under 70 ℃ until the pH value of the suspension arrived 7.0. The suspension was aged for 3h under 70 ℃, followed by centrifugation and washed with deionized water to neutral. The resulting product was dried under 110 ℃ for 12h and calcined under 500 ℃ for 1h under static air. The catalyst was denoted as Zn-Cr-1.5-1, which means the molar ratio of Zn/Cr atom is 1.5:1. The catalyst containing Al was denoted as Zn-Cr-Al-3.5-1-1, which means the molar ratio of Zn/Cr/Al atom is 3.5:1:1.

SAPO-34 was synthesized hydrothermally [13]. 85% H_3PO_4 and 35% TEAOH was added to deionized water under continuous stirring. Subsequently, 30% silica sol was added dropwise into the solution, followed by addition of aluminium isopropoxide in small quantity. After vigorous stirring for 1h, 35% hydrochloric acid was added dropwise. The mixture was transferred into a 200-mL Teflon-lined stainless steel autoclave after intense stirring for 1 h. The hydrothermal synthesis proceeded under 190 ℃ for 32h with rotation. After centrifugation and washing, the solid product was dried under 110 ℃ for 12h and calcined under 550 ℃ for 3h under flowing

Yuxuan Huang, Weixin Qian, Hongfang Ma, Haitao Zhang, and Weiyong Ying are with Engineering Research Center of Large Scale Reactor Engineering and Technology, East China University of Science and Technology, Shanghai 200237, China (e-mail: xinshouxuanxuan@163.com, wxqian@ecust.edu.cn, mark@ecust.edu.cn, zht@ecust.edu.cn, wying@ecust.edu.cn).

air.

B. Catalytic Performance Test

Catalytic reactions were performed in a fixed-bed stainless steel reactor with a quartz lining. $ZnCrO_x$ oxide and SAPO-34 were both dried by a far-infrared dryer before being weighed. 150 mg $ZnCrO_x$ oxide (250-425 μm) and SAPO-34 with same weight and size were mixed in a centrifuge tube. After vigorous shaking, 300-mg composite catalyst was sent into the reactor. The composite catalyst was reduced in situ in H_2 under 310 ℃ for 3 h. Catalytic reaction was carried out under 380 ℃, 1MPa, $H_2/CO/N_2$=60/30/10 and GHSV=6000 $mL \cdot g_{cat}^{-1} \cdot h^{-1}$. Products were analyzed by an online Agilent 7890A GC. The catalytic performance after 800 minutes of reaction was used for discussion. The carbon balance was over 99%. The calculation of CO conversion was below.

$$X_{CO} = \frac{CO_{\text{in}} - CO_{out}}{CO_{in}} \times 100\%$$

where CO_{in} and CO_{out} represent molar flow of CO at the inlet and outlet, respectively.

The calculations of selectivity to CO_2 and hydrocarbons were below.

$$S_{CO_2} = \frac{CO_{2,out}}{CO_{in} - CO_{out}} \times 100\%$$

where $CO_{2,out}$ represents molar flow of CO_2 at the outlet.

$$S_{C_nH_m} = \frac{nC_nH_{m,out}}{\sum nC_nH_{m,out}} \times 100\%$$

where $C_nH_{m_{out}}$ represents molar flow of C_nH_m at the outlet.

C. Characterization

XRD was performed on a Bruker D8 Advance X-ray polycrystalline diffractometer with Cu Kα radiation at 40 kV and 40 mA in the range of 2θ=5-80°.

N_2 adsorption-desorption was carried out at -196 ℃ on a micromeritics ASAP 2020. All samples were degassed under vacuum at 350 ℃ for 6h before analysis. The micropore volume was calculated by t-plot method.

NH_3-TPD was carried out on a micromeritics AutoChem II 2920. 0.1 g sample was pretreated in flowing He at 600 ℃ for 30 minutes. After cooling down to 60 ℃ under flowing He, the adsorption of 10%NH_3 in He was proceeded under 60 ℃ for 30 minutes. Then, He flow was used to purge excess NH_3 for 30 minutes until a stable baseline was obtained. At last, signal was recorded when the temperature was increased from 60 ℃ to 800 ℃ at a heating rate of 10 ℃/min under flowing He.

H_2-TPR was carried out on a micromeritics AutoChem II 2920. 0.05 g sample was pretreated in flowing Ar at 400 ℃ for 60 minutes. After cooling down to 60 ℃ under flowing Ar until a stable baseline was obtained, 10%H_2 in Ar was used to proceed reduction. Signal was recorded when the temperature was increased from 60 ℃ to 800 ℃ at a heating rate of 10 ℃/min under flowing Ar.

CO-TPD was carried out on a micromeritics AutoChem II 2920. At first, 0.25g sample underwent in situ reduction with H_2 at 310 ℃ for 3 hours. After cooling down to 60 ℃ under flowing He, the adsorption of carbon monoxide was proceeded under 60 ℃ for 30 minutes. Then, He flow was used to purge excess CO for 30 minutes until a stable baseline was obtained. At last, signal was recorded when the temperature was increased from 60 ℃ to 800 ℃ at a heating rate of 10 ℃/min under flowing He.

III. Results and Discussion

A. XRD

XRD patterns showed that Zn-Cr-0.5-1 was composed of pure $ZnCr_2O_4$ spinel structure since the characteristic peaks of ZnO were negligible (Fig. 1 (b)). Zn-Cr-1.5-1 to Zn-Cr-4.5-1 were composed of ZnCr2O4 and ZnO. The addition of Zn introduced ZnO, and ZnO became dominant along with the addition of Zn. The addition of Al to Zn-Cr-3.5-1 widened the peak, which indicated that Al can decrease the particle size as structure promoter. Meanwhile, neither $ZnAl_2O_4$ nor Al_2O_3 was observed on the XRD pattern of Zn-Cr-Al-3.5-1-1, which might be due to the low content of Al.

XRD pattern of SAPO-34 was shown in Fig. 2. The synthesized SAPO-34 exhibited the typical XRD patterns of zeolites with the chabazite (CHA) framework topology.

B. Catalytic Performance

Considering the XRD result and catalytic performance, the metal oxide samples can be divided into $ZnCrAlO_x$ (Zn-Cr-Al-3.5-1-1) and $ZnCrO_x$, and $ZnCrO_x$ can be divided into $ZnCr_2O_4$ (Zn-Cr-0.5-1) and ZnO-$ZnCr_2O_4$ (Zn-Cr-1.5-1 to Zn-Cr-4.5-1). Fig. 3 showed the catalytic performance of bifunctional catalyst for direct conversion of syngas to light olefins. From the comparison between Zn-Cr-0.5-1 and Zn-Cr-1.5-1, it can be concluded that the addition of ZnO to $ZnCr_2O_4$ can significantly increase the CO conversion, while CH_4 selectivity decreased and light olefins selectivity increased obviously. The olefins/paraffins ratio also increased.

As the Zn/Cr ratio increased in ZnO-$ZnCr_2O_4$, CO conversion decreased slightly, while CH_4 and C_{5+} selectivity increased, and light olefins selectivity decreased slightly as well. However, the olefins/paraffins ratio decreased obviously.

The addition of Al to Zn-Cr-3.5-1 led to a noteworthy increase to CO conversion. CH_4 and C_{5+} selectivity decreased, while both light olefins selectivity and olefins/paraffins ratio increased.

On the basis of these data, it can be concluded that there exists an optimal Zn/Cr ratio for bifunctional catalyst. Among the samples that we have prepared, the best Zn/Cr ratio is 1.5. 14% CO conversion, 3.9% CH_4 and 85.68% light olefins among hydrocarbons were achieved under 380 ℃, 1 MPa, H_2/CO=2, GHSV=6000 $mL \cdot g_{cat}^{-1} \cdot h^{-1}$, TOS=800 min.

Furthermore, the addition of Al promotes the catalytic performance notably. Details will be discussed below with NH_3-TPD, N_2 adsorption-desorption, H_2-TPR, and CO-TPD.

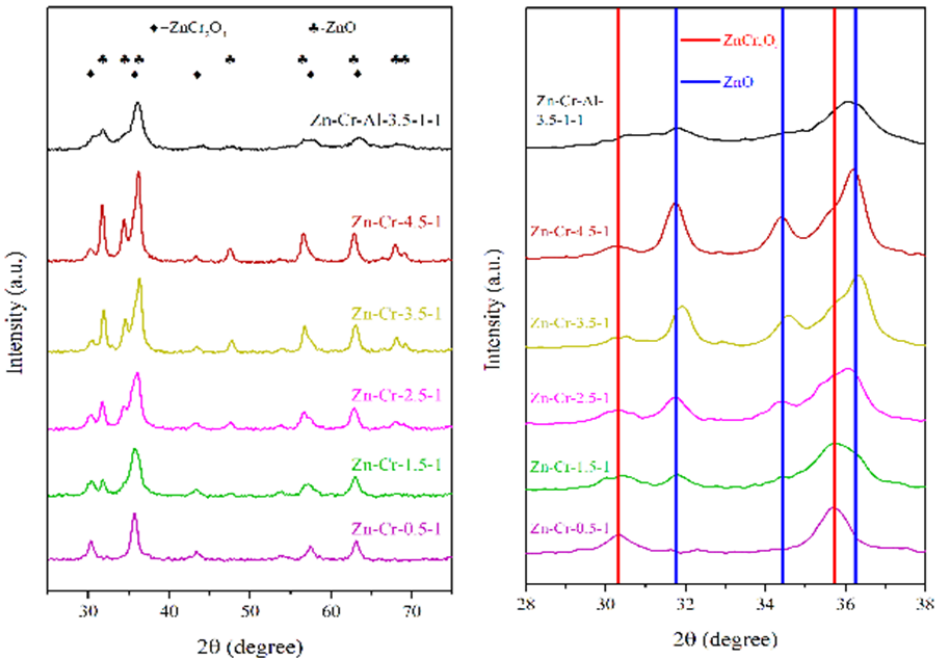

(a) (b)

Fig. 1 XRD patterns of metal oxides (a) 2θ=25-75° (b) 2θ=28-38°

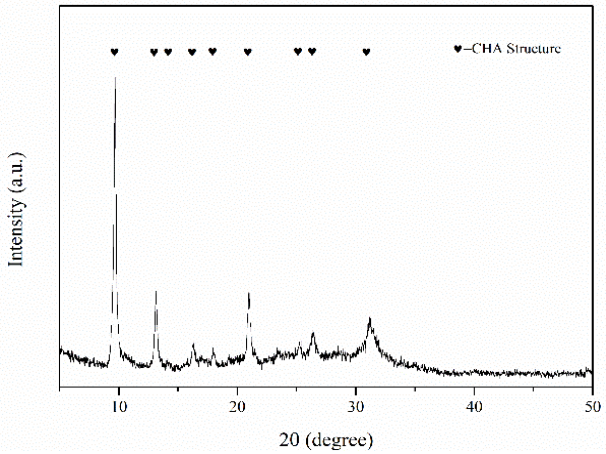

Fig. 2 XRD pattern of the synthesized SAPO-34

C. NH_3-TPD

NH_3-TPD profile showed the acid property of the synthesized SAPO-34 (Fig. 3). The peak at the lower temperature (137 ℃ in this case) has been proven to be related to a weakly held ammonia, which may be adsorbed by hydrogen bond, but not the ammonia species adsorbed on the acid site. The peak at the higher temperature (347 ℃ in this case) is widely used to characterize strong acid site in zeolite [14], [15]. Compared with the literature [5], SAPO-34 that we have synthesized exhibited a rather weak strong acid. Therefore, the hydrogen transfer reaction was suppressed, leading to the high light olefins selectivity among most of the catalytic performance tests.

Since all the catalytic performance tests used the same SAPO-34, the difference of $C_{2\text{-}4}^{=}/C_{2\text{-}4}^{o}$ among the results should not be ascribed to the acid property of SAPO-34.

D. N_2 Adsorption-Desorption

The textural properties of metal oxides and SAPO-34 were shown in Table I. BET surface area of $ZnCrO_x$ became slightly smaller along with the addition of Zn, but the difference is insignificant. The pore volume was similar among $ZnCrO_x$ with varying Zn/Cr ratio. Hence, the impact of Zn/Cr ratio on the textural properties of catalysts should not be a key factor to the difference in catalytic performance. However, CO conversion increased from 12.81% to 15.99% as the addition of Al doubled BET surface area and pore volume. The impact of Al was noteworthy. Al played the role of structure promoter and increased the surface area of metal oxide, leading to more $ZnCr_2O_4$ being exposed to the surface rather than in bulk phase. It directly increased active sites for CO activation and influenced the chemisorption property.

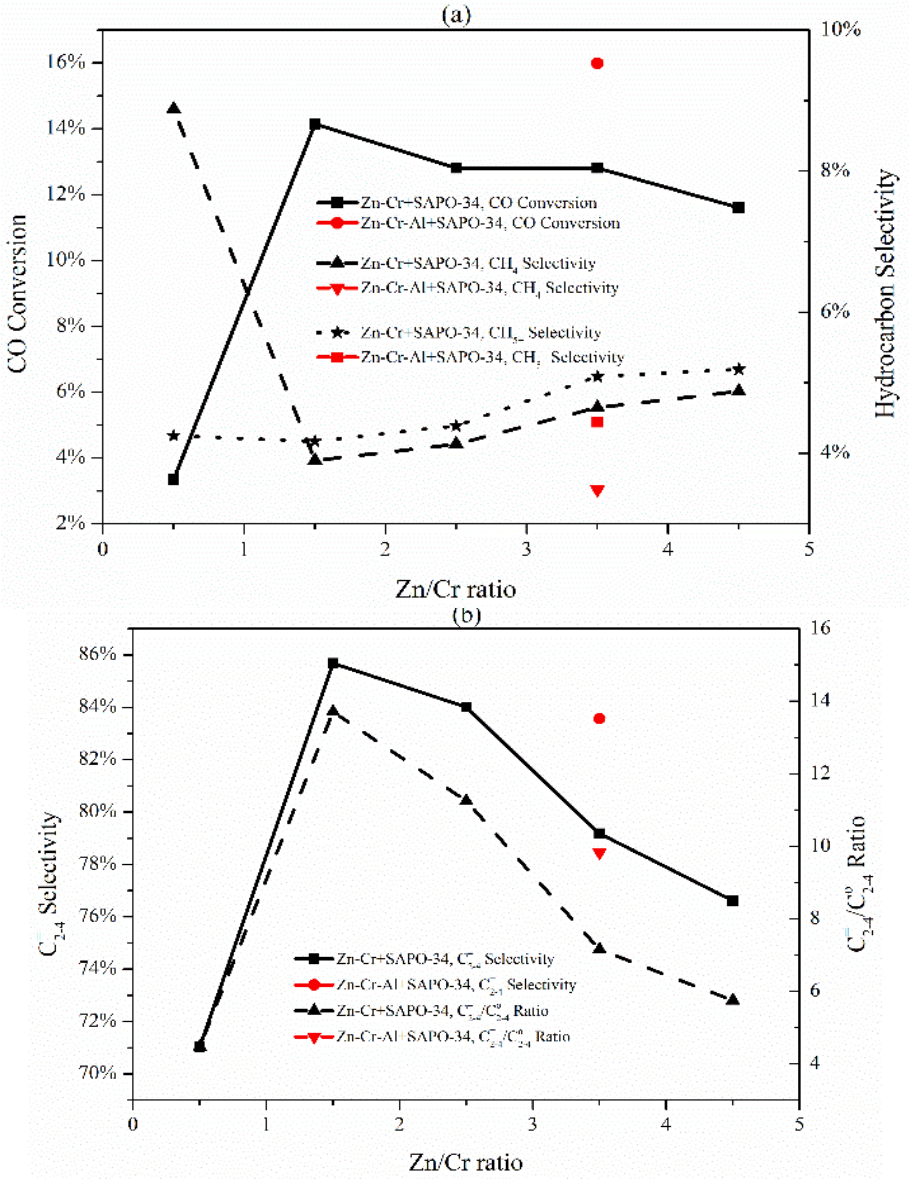

Fig. 3 Catalytic performance of bifunctional catalysts (a) CO conversion, CH_4 selectivity and C_{5+} selectivity (b) Light olefins selectivity and Olefins/paraffins ratio of C_{2-4} hydrocarbon

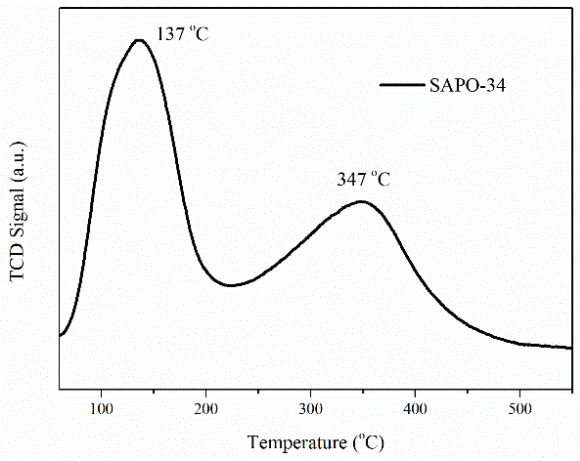

Fig. 4 NH_3-TPD pattern of the synthesized SAPO-34

TABLE I
TEXTURAL PROPERTIES FOR METAL OXIDES AND SAPO-34

Sample	BET Surface Area (m^2/g)	V_{total} (cm^3/g)	V_{micro} (cm^3/g)	V_{meso}/V_{total} (%)
Zn-Cr-0.5-1	66.77	0.25	0.00	100
Zn-Cr-1.5-1	65.85	0.30	0.00	100
Zn-Cr-2.5-1	62.29	0.28	0.00	100
Zn-Cr-3.5-1	60.27	0.27	0.00	100
Zn-Cr-4.5-1	57.41	0.27	0.00	100
Zn-Cr-Al-3.5-1-1	120.66	0.54	0.00	100
SAPO-34	487.59	0.44	0.23	47.15

The synthesized SAPO-34 exhibited hierarchical pore structure, which is a benefit to achieve higher reaction activity and more resistive to carbon deposition compared with conventional SAPO-34. Combined with the rather weak strong acid and moderate acid amount of zeolite and the optimized

metal oxide, CO conversion was much higher than other reports under similar reaction condition [6], [7].

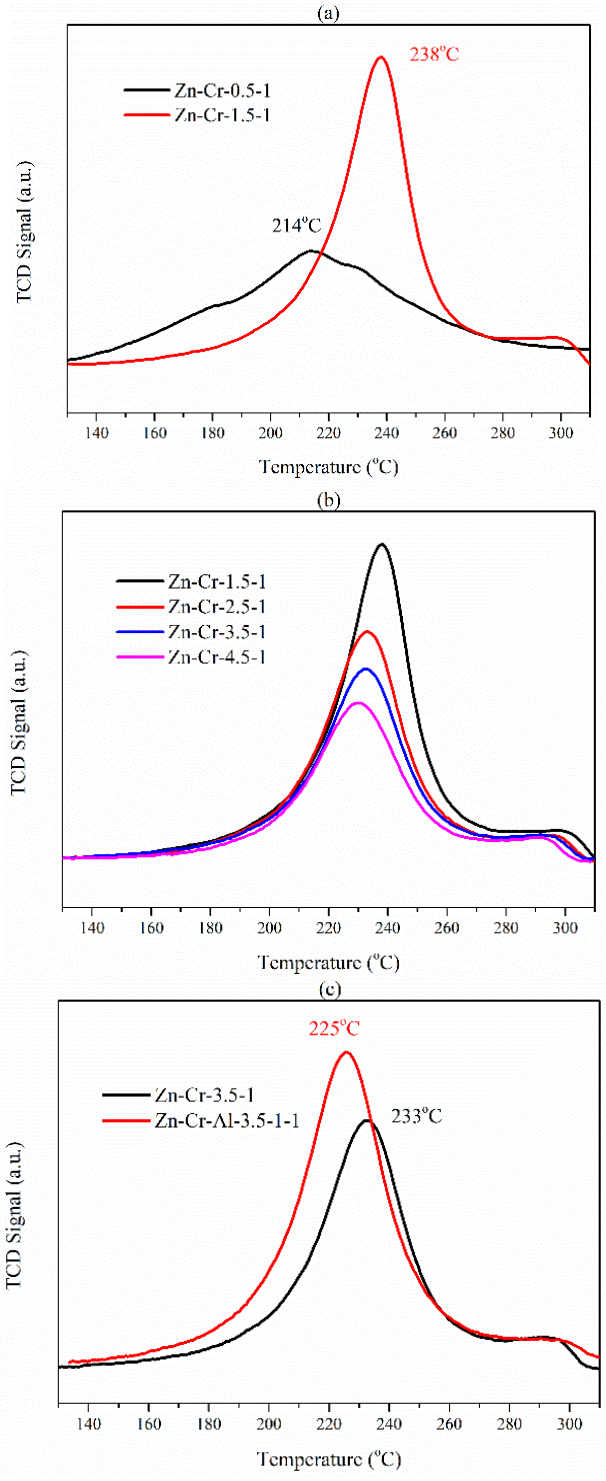

Fig. 5 H_2-TPR patterns of the metal oxides (a) Zn-Cr-0.5-1 and Zn-Cr-1.5-1 (b) Zn-Cr-1.5-1 to Zn-Cr-4.5-1 (c) Zn-Cr-3.5-1 and Zn-Cr-Al-3.5-1-1

E. H_2-TPR

During the reduction process, several oxygen vacancies were generated on the surface of $ZnCr_2O_4$ spinel, and such surface with oxygen vacancies was the site for CO activation [5]. The peak temperature for Zn-Cr-0.5-1 was much lower than Zn-Cr-1.5-1 (Fig. 5 (a)), which meant that the addition of ZnO hindered the reduction of $ZnCr_2O_4$, but the chosen temperature (310 °C) for H_2 reduction before the catalytic performance tests was capable of completing the reduction. The peaks for ZnO-$ZnCr_2O_4$ were sharper than the peak for pure $ZnCr_2O_4$ spinel, which indicated that ZnO facilitated to uniform the reductibility of $ZnCr_2O_4$. ZnO-$ZnCr_2O_4$ with different Zn/Cr ratio showed similar peak temperature and distribution (Fig. 5 (b)), indicating the similar reduction behavior among these samples. From the quantitative analysis listed in Table II, H_2 consumption decreased along with the addition of ZnO, owing to the mass fraction of ZnO, which is unreducible by H_2, increased. To subtract dilution effect caused by ZnO, H_2 consumption based on $ZnCr_2O_4$ was calculated, and H_2 consumption based on $ZnCr_2O_4$ increased along with the addition of ZnO, suggesting that ZnO facilitated to make full use of $ZnCr_2O_4$ despite that ZnO- $ZnCr_2O_4$ was slightly harder to be reduced than pure $ZnCr_2O_4$ spinel and ZnO decreased $ZnCr_2O_4$ mass fraction. Hence, there should be an optimal ZnO content. Zn-Cr-1.5-1 showed the highest H_2 consumption and a rather high H_2 consumption based on $ZnCr_2O_4$, and it showed the best catalytic performance.

The addition of Al to Zn-Cr-3.5-1 increased H_2 consumption and decreased peak temperature at the same time (Fig. 5 (c)), which can be related to the rise of surface area and pore volume. The improvement of reduction behavior also resulted in the better catalytic performance.

TABLE II
QUANTITATIVE RESULTS OF H_2-TPR

Sample	H_2 consumption (mmol/g)	$ZnCr_2O_4$ mass fraction	H_2 consumption (mmol/g $ZnCr_2O_4$)
Zn-Cr-0.5-1	0.57	1.00	0.57
Zn-Cr-1.5-1	0.78	0.59	1.33
Zn-Cr-2.5-1	0.61	0.42	1.47
Zn-Cr-3.5-1	0.53	0.32	1.64
Zn-Cr-4.5-1	0.45	0.26	1.71
Zn-Cr-Al-3.5-1-1	0.63	0.25	2.23

F. CO-TPD

Since $ZnCr_2O_4$ surface with oxygen vacancies is the site for CO activation, CO-TPD after in situ H_2 reduction was carried out to investigate CO adsorption behavior. Fig. 6 (a) showed the CO-TPD profiles between Zn-Cr-0.5-1 and Zn-Cr-1.5-1. The desorption peak temperature was similar at the range of lower than 300 °C. But, the decline of the peak temperature at high temperature range revealed that the interaction between CO and $ZnCr_2O_4$ surface with oxygen vacancies was weakened with the addition of ZnO. The textural properties of Zn-Cr-0.5-1 and Zn-Cr-1.5-1 were similar, so the difference in CO desorption was not caused by textural property. Solo ZnO had a desorption peak at 477 °C, but the amount of CO adsorption on ZnO is negligible. Therefore, the difference in CO desorption was not caused by CO adsorption on ZnO.

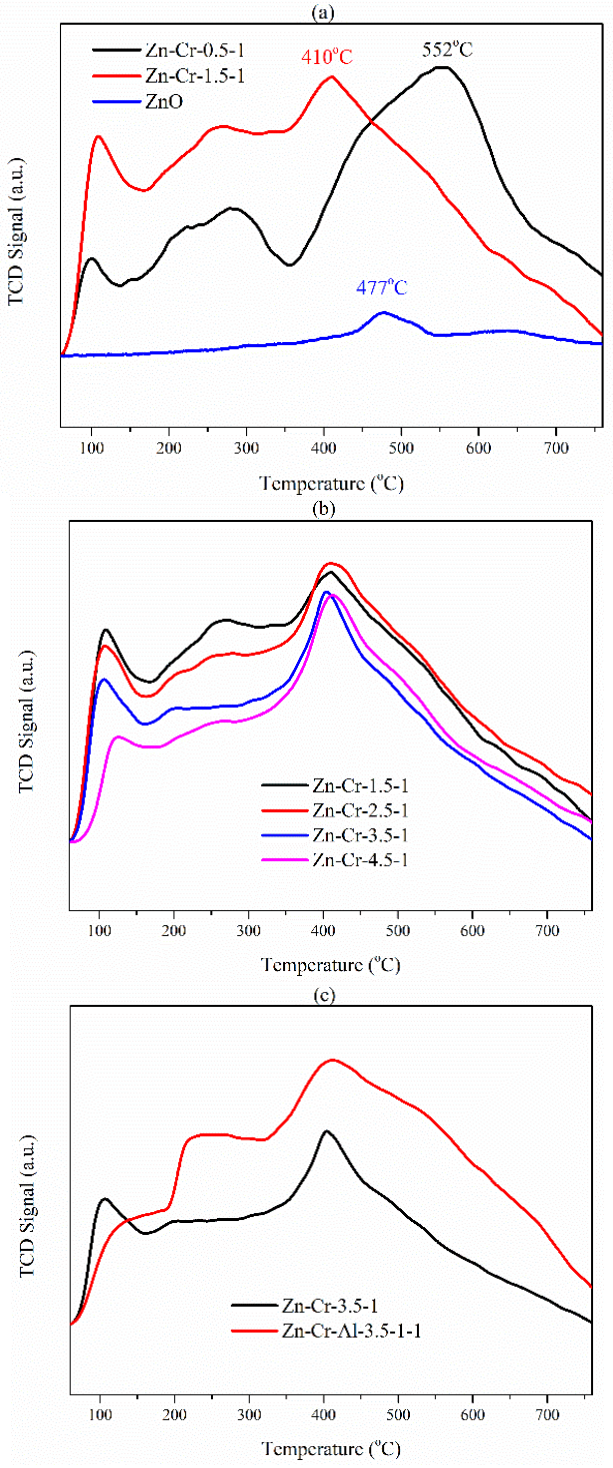

Fig. 6 CO-TPD patterns of the metal oxides (a) Zn-Cr-0.5-1 and Zn-Cr-1.5-1 (b) Zn-Cr-1.5-1 to Zn-Cr-4.5-1 (c) Zn-Cr-3.5-1 and Zn-Cr-Al-3.5-1-1

Recently, a DFT research [16] that focused on excess Zn on spinel-structured $ZnCr_2O_4$ showed that the adsorption of CO on $ZnCr_2O_4$ with excess Zn is weaker than on stoichiometric $ZnCr_2O_4$, indicating higher reactivity. The structure was reported to be a thin, amorphous ZnO layer supported on the $ZnCr_2O_4$ spinel. At the higher concentration of incorporated Zn, the oxygen vacancy formation energy decreases, indicating high reducibility of the system. Our experimental results of CO-TPD were in accord with this literature.

CO-TPD profiles among ZnO-$ZnCr_2O_4$ with different Zn/Cr ratio were similar (Fig. 6 (b)), since both the textural structure the surface composition [16] were similar. Fig. 6 (c) showed that the addition of Al had no effect on peak temperature, but increased the amount of CO adsorption, owing to the improvement of textural property. The increased surface area exposed more $ZnCr_2O_4$ to the surface without changing its chemical environment, thus provided more oxygen vacancies to adsorb CO.

IV. Conclusion

A series of Zn-Cr oxides were prepared by coprecipitation and were mixed with SAPO-34 to be used as bifunctional catalyst for direct conversion of syngas to light olefins. The Zn/Cr ratio was found to be a critical factor on the catalytic property, whereas the presence of Al had a crucial influence on the textural and catalytic property. The ideal Zn/Cr ratio among the samples that we prepared was 1.5. It exhibited CO conversion of 14%, light olefins selectivity of 86% when mixed with SAPO-34, while CH_4 selectivity was only 3.9%. $ZnCr_2O_4$ and ZnO-$ZnCr_2O_4$ showed similar textural property but exhibited different catalytic performances when mixed with SAPO-34. H_2-TPR revealed that ZnO facilitated the reduction of $ZnCr_2O_4$, but too much addition of ZnO decreased the portion of $ZnCr_2O_4$. CO-TPD indicated that ZnO significantly weakened the interaction between the adsorbed CO and the surface with oxygen vacancy, which is consistent with the calculation from literature [16]. Zn-Cr-Al-3.5-1-1 exhibited CO conversion of 16%, light olefins selectivity of 84% when mixed with SAPO-34, while CH_4 selectivity was only 3.5%. The addition of Al to ZnO-$ZnCr_2O_4$ did not change the phase components, but improved the textural property, leading to the enhancement of reducibility and chemisorption property to CO, which resulted in a better catalytic performance.

Acknowledgment

This work was supported by the National High-Tech R&D Program of China [2011AA05A204].

References

[1] Hirsa M. Torres Galvis and Krijn P. de Jong, "Catalysts for production of lower olefins from synthesis gas: a review" in *ACS Catalysis*, vol. 3, issue. 9, 2013, pp. 2130–2149.

[2] Zhiqiang Yang, Shujing Guo, Xiulian Pan, Junhu Wang and Xinhe Bao, "FeN nanoparticles confined in carbon nanotubes for CO hydrogenation" in *Energy & Environmental Science*, vol. 4, issue. 11, 2011, pp. 4500–4503.

[3] Zhiqiang Yang, Xiulian Pan, Junhu Wang and Xinhe Bao, "FeN particles confined inside CNT for light olefin synthesis from syngas: effects of Mn and K additives" in *Catalysis Today*, vol. 186, issue. 1, 2012, pp. 121–127.

[4] Hirsa M. Torres Galvis, Johannes H. Bitter, Chaitanya B. Khare, Matthijs Ruitenbeek, A. Iulian Dugulan and Krijn P. de Jong, "Supported iron nanoparticles as catalysts for sustainable production of lower olefins" in *Science*, vol. 335, issue. 3070, 2012, pp. 835–838.

[5] Feng Jiao, Jinjing Li, Xiulian Pan, Jianping Xiao, Haobo Li, Hao Ma, et al., "Selective conversion of syngas to light olefins" in *Science*, vol. 351,

issue. 6277, 2016, pp. 1065–1068.
[6] Xiaoliang Liu, Wei Zhou, Yudan Yang, Kang Cheng, Jincan Kang, Lei Zhang, et al., "Design of efficient bifunctional catalysts for direct conversion of syngas into lower olefins via methanol/dimethyl ether intermediates" in *Chemical Science*, vol. 9, issue. 20, 2018, pp. 4708–4718.
[7] Kang Cheng, Bang Gu, Xiaoliang Liu, Jincan Kang, Qinghong Zhang and Ye Wang, "Direct and highly selective conversion of synthesis gas into lower olefins: design of a bifunctional catalyst combining methanol synthesis and carbon-carbon coupling" in *Angewandte Chemie*, vol. 128, issue. 15, 2016, pp. 4803–4806.
[8] Feng Jiao, Xiulian Pan, Ke Gong, Yuxiang Chen, Gen Li and Xinhe Bao, "Shape-selective zeolites promote ethylene formation from syngas via a ketene intermediate" in *Angewandte Chemie International Edition*, vol. 57, issue. 17, 2018, pp. 4692–4696.
[9] Yifeng Zhu, Xiulian Pan, Feng Jiao, Jian Li, Junhao Yang, Minzheng Ding, et al., "Role of manganese oxide in syngas conversion to light olefins" in *ACS Catalysis*, vol. 7, issue. 4, 2017, pp. 2800–2804.
[10] Xiaoliang Liu, Mengheng Wang, Cheng Zhou, Wei Zhou, Kang Cheng and Jincan Kang, et al., "Selective transformation of carbon dioxide into lower olefins with a bifunctional catalyst composed of ZnGa2O4 and SAPO-34" in *Chemical Communications*, vol. 54, issue. 2, 2018, pp. 140–143.
[11] Junhao Yang, Xiulian Pan, Fengjiao, Jian Li and Xinhe Bao, "Direct conversion of syngas to aromatics" in *Chemical Communications*, vol. 53, issue. 81, 2017, pp. 11146–11149.
[12] Peipei Zhang, Li Tan, Guohui Yang and Noritatsu Tsubaki, "One-pass selective conversion of syngas to para-xylene" in *Chemical Science*, vol. 8, issue. 12, 2017, pp. 7941–7946.
[13] A. Izadbakhsh, F. Farhadi, F. Khorasheh, S. Sahebdelfar, M. Asadi and Z. F. Yan, "Key parameters in hydrothermal synthesis and characterization of low silicon content SAPO-34 molecular sieve" in *Microporous and Mesoporous Materials*, vol. 126, issue. 1-2, 2009, pp. 1–7.
[14] Naonobu Katada, Hirofumi Igi, Jong-Ho Kim and Miki Niwa, "Determination of the acidic properties of zeolite by theoretical analysis of temperature-programmed desorption of ammonia based on adsorption equilibrium" in *The Journal of Physical Chemistry B*, vol. 101, issue. 31, 1997, pp. 5969–5977.
[15] Miki Niwa, Masakazu Iwamoto and Kho-ichi Segawa, "Temperature-programmed desorption of ammonia on zeolites. Influence of the experimental conditions on the acidity measurement" in *Bulletin of the Chemical Society of Japan*, vol. 59, issue. 12, 1986, pp. 3735–3739.
[16] Huiqing Song, Daniel Laudenschleger, John J. Carey, Holger Ruland, Michael Nolan and Martin Muhler, "Spinel-structured ZnCr2O4 with excess Zn is the active ZnO/Cr2O3 catalyst for high-temperature methanol synthesis" in *ACS Catalysis*, vol. 7, issue. 11, 2017, pp. 7610–7622.